Thin films of unsubstituted and fluorinated palladium phthalocyanines: structure and sensor response toward ammonia and hydrogen

PARKHOMENKO, Roman G., SUKHIKH, Aleksander S., KLYAMER, Darya D., KRASNOV, Pavel O., GROMILOV, Sergei A., KADEM, Burak, HASSAN, Aseel <http://orcid.org/0000-0002-7891-8087> and BASOVA, Tamara V.

Published version

PARKHOMENKO, Roman G., SUKHIKH, Aleksander S., KLYAMER, Darya D., KRASNOV, Pavel O., GROMILOV, Sergei A., KADEM, Burak, HASSAN, Aseel and BASOVA, Tamara V. (2017). Thin films of unsubstituted and fluorinated palladium phthalocyanines: structure and sensor response toward ammonia and hydrogen. Journal of Physical Chemistry C, 121 (2), 1200-1209.

Thin films of unsubstituted and fluorinated palladium phthalocyanines: structure and sensor response toward ammonia and hydrogen

Roman G. Parkhomenko,[a] Aleksander S. Sukhikh,[a] Darya D. Klyamer,[a] Pavel O. Krasnov,[a] Sergei A. Gromilov,[a,b] Burak Kadem,[c] Aseel K. Hassan,[c] Tamara V. Basova[a,b]

[a]*Nikolaev Institute of Inorganic Chemistry SB RAS, 3, Lavrentieva Ave., 630090 Novosibirsk, Russia*

[b]*Novosibirsk State University, 2, Pirogova Str., 630090 Novosibirsk, Russia*

[c]*Faculty of Arts, Computing, Engineering and Sciences, Materials and Engineering Research Institute, Sheffield Hallam University, Furnival Building, 153 Arundel Street, Sheffield S1 2NU, United Kingdom*

Abstract

In the present work, we study and compare the structure and sensing properties of thin films of unsubstituted palladium phthalocyanine (PdPc) and hexadecafluorosubstituted palladium phthalocyanine ($PdPcF_{16}$). Thin films of PdPc and $PdPcF_{16}$ were obtained by the method of organic molecular beam deposition and their structure was studied using UV-visible spectroscopy, X-ray diffraction and atomic force microscopy techniques. The electrical sensor response of PdPc films toward ammonia and hydrogen was investigated and compared with that of $PdPcF_{16}$ films. The nature of interaction between the phthalocyanines films and some gaseous analyte molecules has been clarified using Quantum chemical (DFT) calculations.

Keywords: Palladium phthalocyanines; Thin films; Film structure; DFT calculations; Chemiresistive sensors

1. Introduction

Phthalocyanines (Pc) are class of N_4-macrocycles containing π-electron systems with 18 electrons. These compounds have been the subject of studies for various applications due to their high stability, intriguing optical and electrical characteristics, sensor properties and so on [1]. Among other phthalocyanines, palladium phthalocyanine (PdPc) is known as a p-type semiconductor with charge carriers (holes) mobility of $2.5x10^{-5}cm^2/Vs$ [2]. Moreover PdPc exhibits longer exciton diffusion length in comparison with other bivalent metal phthalocyanines, such as ZnPc and CuPc [3]. This property as well as the strong absorption within the visible spectral range makes PdPc films a quite useful candidate for photovoltaic applications [4, 5]. Thin films of palladium phthalocyanine have also demonstrated good sensing properties for different gaseous analytes, with fast response times, high base line stability and enhanced sensitivity. Recent studies showed that films of PdPc can be used as active layers of chemical sensors for the determination of humidity [6], oxygen [7], ammonia and NO_2 [8].

Bilayer film structures consisting of palladium and various phthalocyanines are used as sensor layers for the detection of hydrogen [9-11]. In these structures the palladium layer is responsible for the high permeability and selectivity for hydrogen [12], while MPcs demonstrate good sensor response. Jakubik et al. [9] have shown that bilayer structures consisting of Pd and H_2Pc demonstrate improved sensor performance in comparison with a single palladium layer.

It is well known that substitution of functional groups at the periphery of benzene ring leads to different structures of the films leading to different electrical and sensing properties of these films [13, 14]. For instance, the introduction of electron-withdrawing fluorine substituents to MPc (M=Cu(II), Zn(II)) decreases the electron density of the conjugated macrocycle and increases the oxidation potential of the molecule [15, 16]. This makes fluorine substituted phthalocyanines possessing more sensitivity to the reducing gases like NH_3 and H_2 as compared to unsubstituted analogues [13, 14, 17]. Although the structural features and sensor response of

some fluorosubstituted M(II)Pc (e.g., CuPc, ZnPc, CoPc) were studied in details [14, 18-21], much less seems to be known about fluorosubstituted palladium phthalocyanines.

In the present work, we study and compare the structure and sensor response of thin films of unsubstituted (PdPc) and hexadecafluorosubstituted ($PdPcF_{16}$) palladium phthalocyanines. Thin films of PdPc and $PdPcF_{16}$ were obtained by means of organic molecular beam deposition (OMBD) and their structure was studied using UV-visible spectroscopy, X-ray diffraction (XRD) and atomic force microscopy (AFM) techniques. The electrical sensor response of the palladium phthalocyanine films toward ammonia and hydrogen was investigated and compared with that of hexadecafluorosubstituted palladium phthalocyanine films. Quantum chemical (DFT) calculations have been employed for further in depth understanding the nature of interaction between phthalocyanines and the analyte molecules.

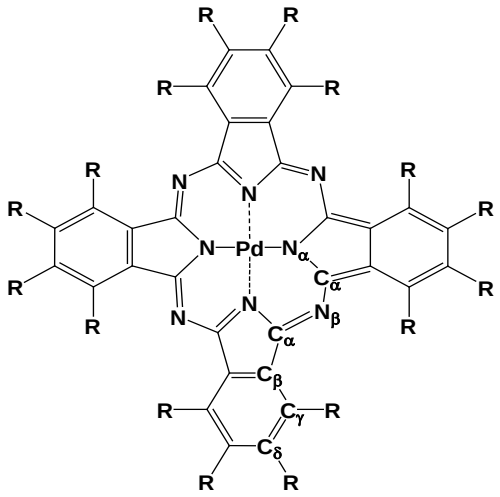

Figure 1. Scheme of PdPc (R=H) and $PcPcF_{16}$ (R=F).

2. Experimental details

2.1. Materials

Unsubstituted (PdPc) and hexadecafluorosubstituted ($PdPcF_{16}$) palladium phthalocyanines were synthesized by heating an equimolar 1:4 mixture of palladium chloride with 1,2-dicyanobenzene and tetrafluorophthalonitrile (Sigma-Aldrich), respectively, in glass tubes for a period of 6-7 hours at 220 ^{o}C. The reaction products were then washed with ethanol and acetone to remove

soluble organic admixtures. All synthesized PdPc species were purified by gradient sublimation in vacuum (10^{-5} Torr) at 440-460 ^{o}C.

2.2. Deposition and characterization of thin films

Thin films of palladium phthalocyanines were obtained by organic molecular beam deposition at room temperature under vacuum of 10^{-5} Torr with the deposition rate of 0.6 nm·s^{-1}. The nominal thickness of the films was about 120 nm. The substrates were varied according to the particular experimental requirements. Glass slides were employed as substrates for spectral and microscopic measurements, while silicon substrates were used for atomic force microscopy (AFM) using a Nanoscope IIIa (Veeco Instruments, Plainview, U.S.A.) to study films' morphology. UV-Vis spectra of MPc solutions as well as films deposited on quartz substrates were recorded using a UV–Vis-3101PC ‘‘Shimadzu” spectrophotometer. IR spectra were recorded using a Vertex 80 FTIR spectrometer. Raman spectra were recorded with a Triplemate SPEX spectrometer equipped with CCD detector in a back-scattering geometry. The 488 nm, 100 mW line of an Ar-laser was used for spectra excitation.

X-Ray diffraction measurements of PdPc and $PdPcF_{16}$ polycrystalline powders and thin layers were performed using Shimadzu XRD-7000 powder X-ray diffractometer (CuKα, 40kV 30mA, Bragg-Brentano geometry, θ-θ goniometer, R = 200 mm, scintillation counter) in the range from 3 to 40° (step 0.03°, integration time 40 s per step). Polycrystalline corundum was used as a standard. 2D Grazing Incidence X-Ray Diffraction (2D GIXD) measurements were carried out on Bruker Duo single crystal X-ray diffractometer (CuKα, 45kV 0.64mA, Incoatec IμCu microfocus source, 0.6 mm collimator, 1024x1024 pixel flat CCD detector); samples were mounted on the goniometer head as described by Sukhikh *et al.* [22]. The primary beam angle of incidence was in the range from 0 to 1°. Distance from the sample to the CCD detector was 80 mm.

2.3. Quantum chemical calculations

Stability of the complexes and characteristics of interaction of NH_3 and H_2 with PdPc and $PdPcF_{16}$ were estimated with the density functional theory (DFT) using the BP86/def2-SVP method [23-26] and Grimme D3 dispersion correction [27, 28]. The ORCA suite of quantum chemical programs was used for all calculations [29].

At the first stage, the geometries of molecules were optimized without symmetry restrictions and with spin multiplicities equal to 1. The binding parameters of NH_3 with PdPc and $PdPcF_{16}$ were then estimated as described elsewhere [14]. Similar estimation was applied in the case of phthalocyanines interaction with H_2, but with a preliminary step when possible orientations of hydrogen molecule relative to PdPc and $PdPcF_{16}$ were analyzed. Taking into account the zero value of H_2 dipole moment, since hydrogen atoms are linked by covalent non-polar bond, a weak interaction of this molecule with palladium atom of phthalocyanines is expected. From this point of view three possible orientations of H_2 relative to PdPc and $PdPcF_{16}$ (Fig. 2) are most probable. If the phthalocyanine molecule is placed in *xy* plane, with the central metal atom position coincides with the origin of the coordinates, then the hydrogen molecule is situated above this plane, when the mass center of H_2 has a place on the *z* axis. In the case of P_1 and P_2 orientations the hydrogen molecule is parallel to the *xy* plane with a different direction relative to *z* axis; in the case of *V* orientation both hydrogen atoms are located along the *z* axis. The dependence of interaction energy E_i of H_2 with the corresponding phthalocyanines on the distance d(Pd-H_2) between palladium atom and mass center of the hydrogen molecule was estimated. For that reason the preliminary geometry optimization of all compounds separately was carried out, and later the calculations of total energy of $PdPcF_x\cdots H_2$ system, where x = 0 or 16, were performed at the different distances between Pd atom and H_2 molecule. Herein the locations of hydrogen atoms were varied along the *z* axis on the condition that their positions along two other axes as well as positions of all other atoms were invariable.

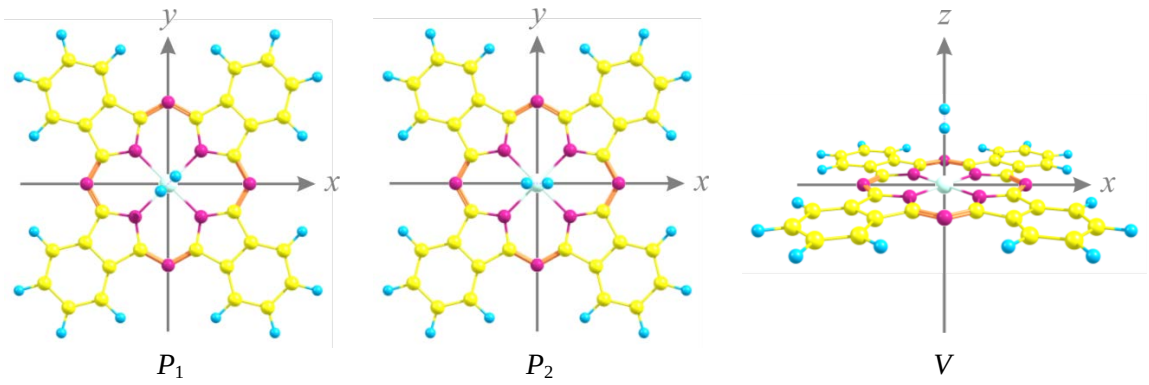

Figure 2. Orientations of hydrogen molecule relative to PdPc molecule

2.4. Study of sensor properties

The sensing performance of PdPc and $PdPcF_{16}$ thin films was studied in response to ammonia (10-50 ppm) and hydrogen (1000-5000 ppm) diluted with air. Pure commercial NH_3 and H_2 gases were used as analyte sources. The injection of gas analytes (NH_3 or H_2) was carried out at a constant flow rate of 300 ml/min and the exposure time was fixed at 10 s in the case of ammonia and 20 s in the case of hydrogen for all examined films. Such a dynamic process rather than a static process was used in order to avoid the irreversible occupation of sites of the active sensor layer as it sometimes occurs when the material is exposed over long durations. The phthalocyanine films were deposited onto platinum interdigitated electrodes (DepSens, Spain) to investigate their conductivity changes upon interaction with the gaseous analytes. The electrical resistance of the films was measured using Keithley 236 electrometer by applying a constant dc voltage of 8 V.

3. Results and Discussion

3.1. Films characterization

Fig. 3 shows the electronic absorption spectra of as-deposited PdPc and $PdPcF_{16}$ films. The thickness of the investigated films was about 120 nm. The Q-band in the UV-Vis spectrum of PdPc film splits into two bands with maxima at 620 and 665 nm. This splitting known as Davydov splitting is due to the interaction between crystallographically inequivalent molecules.

It is typical for oblique orientation of transition dipoles [30] and usually observed in the spectra of unsubstituted M(II)Pc (M=Cu, Co, Ni etc.) films characterized by herringbone arrangement of phthalocyanine molecules [31]. Similar spectrum containing the higher energy peak at 613nm and the lower energy peak at 667 nm has been obtained by Jafari *et al.* [8] for 50 nm PdPc films deposited at the substrate temperature of 25 ^{o}C and deposition rate of 0.5–1.0 Å/s.

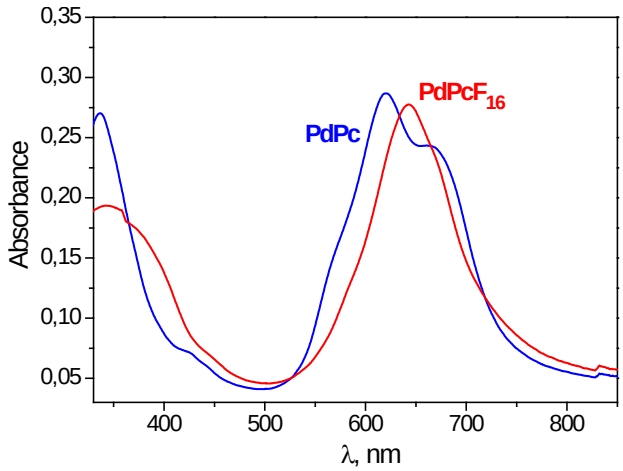

Figure 3. Optical absorption spectra of palladium phthalocyanine films deposited on quartz substrates.

In contrast to PdPc, the film of $PdPcF_{16}$ exhibits a Q-band with one maximum at 643 nm. Such a spectrum with unsplitted Q band was observed only for ultrathin (0.7-1 nm) $ZnPcF_{16}$ films deposited on quartz glass and points toward a cofacial parallel arrangement of chromophores [32, 33]. Thicker films of $MPcF_{16}$ (M=Cu(II), Co(II), Zn(II)) usually exhibits absorption bands located at about 650 and 770 nm [14, 20, 33-35], where the lower energy absorption band shows a maximum in intensity. In general a bathochromic shift of the absorption band relative to the absorption of the solution is characteristic for a “head-to-tail” arrangement of chromophores [30].

Fig. 4 shows diffraction patterns from polycrystalline powders and thin films of PdPc and $PdPcF_{16}$, obtained in the angle range 3° to 40°. Diffraction patterns from powder and thin layers of the two investigated compounds compounds are superimposed on the same graph. Diffraction patterns for thin films are shown with x20 magnification in the range of 2θ from 10° to 40° in

order to display the low-intensity diffraction peaks. Polycrystalline samples were prepared as thin layers on the smooth surface of the standard sample holder made of fused quartz. The metastable α-PdPc phase described by Kempa and Dobrowolski is identified here from the positions of the strongest diffraction peaks on the 2θ axis of the PdPc powder diffraction pattern [36]; however, unit cell parameters were not provided by the authors of the latter reference. In the current work we have successfully managed to index the diffraction pattern (FOM F_{48} = 28.28) in the triclinic unit cell, with the refinement of unit cell parameters performed on 48 single reflections. The resulting unit cell parameters for α-PdPc are: a = 12.19(8) Å; b =3.74(3) Å; c = 13.8(1) Å; α = 107.42(1)°; β = 96.84(1)°; γ = 81.39(1)°; V = 591.74 $Å^3$. No unindexed lines are observed in the diffraction pattern, indicating that the obtained PdPc powder is single-phased. Diffraction pattern from α-PdPc thin layer shows a single high-intensity diffraction peak corresponding to the (001) crystal plane. Low-intensity peaks (I/I_{max} <1%) from 00l plane series and from the (-201) and (102) planes are also observed. Absence of the reflections from the other planes indicates that the thin layers have a strong preferred orientation, with the plane (001) oriented parallel to the substrate plane.

The diffraction pattern from the polycrystalline $PdPcF_{16}$ sample (Fig. 4) is significantly different from α-PdPc, indicating a significant change in its crystal structure. 34 single diffraction lines were observed on the $PdPcF_{16}$ diffraction pattern, but the direct search of the unit cell parameters using Dicvol and Treor algorithms [37, 38] did not yield any meaningful results, which may indicate the possibility that $PdPcF_{16}$ powder contains multiple crystal phases.

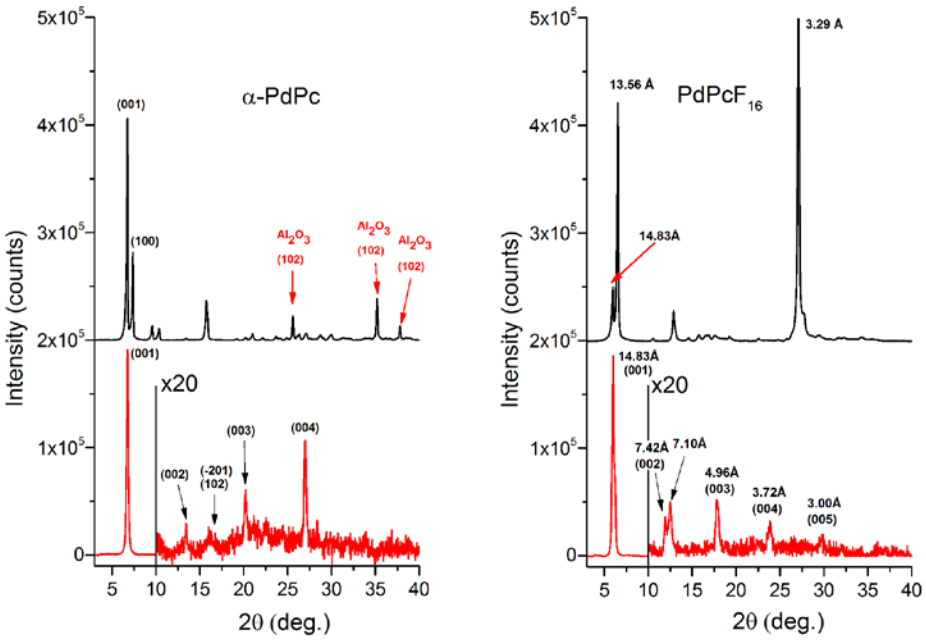

Figure 4. The diffraction patterns of powders (upper black curves) and thin layers (lower red curves) for α-PdPc and $PdPcF_{16}$. The lower curves are shown with x20 magnification in the 2θ range 10° to 40°. The lines marked with red arrows are the corundum lines (used as internal standard).

The XRD pattern obtained from $PdPcF_{16}$ thin layers is represented by a series of diffraction reflections with aliquot interplanar spacing (14.83 Å, 7.42 Å, 4.96 Å, 3.72 Å and 3.00 Å) that allows us to identify them as reflections from series of planes and to attribute the indexes (001), (002), (003), (004) and (005), respectively. This pattern indicates that the crystallites in the $PdPcF_{16}$ thin layers are preferentially oriented relative to the substrate surface.

Fig. 5 shows diffraction patterns of thin layers of α-PdPc and $PdPcF_{16}$, obtained on a Bruker Duo using 2D GIXD technique. Freestanding diffraction spots can be observed on all diffraction patterns, that supports the earlier conclusion about the preferential orientation of crystallites relative to the substrate surface. Based on the previously acquired unit cell parameters, hkl indexes were assigned to the corresponding diffraction spots, as shown in Fig. 5. Like in the case of powder diffraction patterns, the 2D GIXD pattern of $PdPcF_{16}$ is significantly different from α-PdPc. The angle between the planes 001 and 100 (and between their respective diffraction spots in Fig. 5a) is 85.48° for PdPc, while for $PdPcF_{16}$ angle between the corresponding diffraction spots is 59.32°.

Interplanar distances for $PdPcF_{16}$, measured directly by the positions of the observed diffraction spots are given on Fig. 5b. In addition to three orders of reflections from the (00l) plane series, there are two reflections with d = 14.14 Å and d = 7.07 Å, which can be assigned as reflections from (100) and (200) planes, respectively. It is particularly noteworthy that the diffraction peak with d = 14.14 Å is not observed on the $PdPcF_{16}$ powder diffraction pattern. At the same time, the high-intensity diffraction peak at d = 13.56 Å, which is visible on the powder diffraction pattern is not observed on the 2D GIXD pattern. This indicates that polycrystalline $PdPcF_{16}$ sample likely contains two phase modifications of this compound. This circumstance did not allow us to index the powder diffraction pattern.

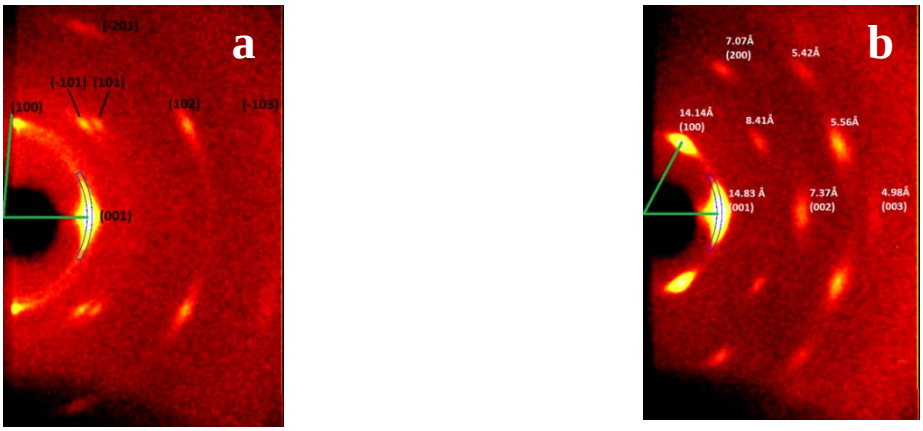

Figure 5. The diffraction patterns of (a) α-PdPc and (b) $PdPcF_{16}$ thin films, obtained by 2D GIXD technique.

Diffraction spot profiles obtained in the Psi-scan mode, corresponding to the reflections from the plane 001, are shown in Fig. 6. It is evident that for both samples the maximum of the diffraction peak is at 0° Psi, which means that the crystallites are arranged with 001 plane parallel to the substrate surface, and for the majority of the crystallites the deviation is no more than 10°.

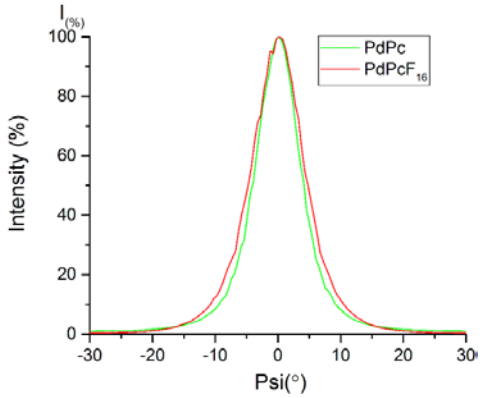

Figure 6. Profile of 001 diffraction peak for each of the diffraction patterns obtained by integrating in the Psi-scan mode in the range of 2θ (±0.2°) of the position of its maximum (the region of integration is highlighted in blue outline on the 2D GIXD diffraction patterns).

The surface morphology of thin films of palladium phthalocyanine was examined using AFM (Fig. 7). As can be clearly seen the as-deposited PdPc film (Fig. 7a) has granular structure with a grain size of 150–220 nm. The *rms* roughness of the film is 16.9 nm. The surface of the $PdPcF_{16}$ film (Fig. 7b) is covered with slightly elongated particles with much smaller sizes. The $PdPcF_{16}$ film has smoother surface with the *rms* roughness of 4.3 nm.

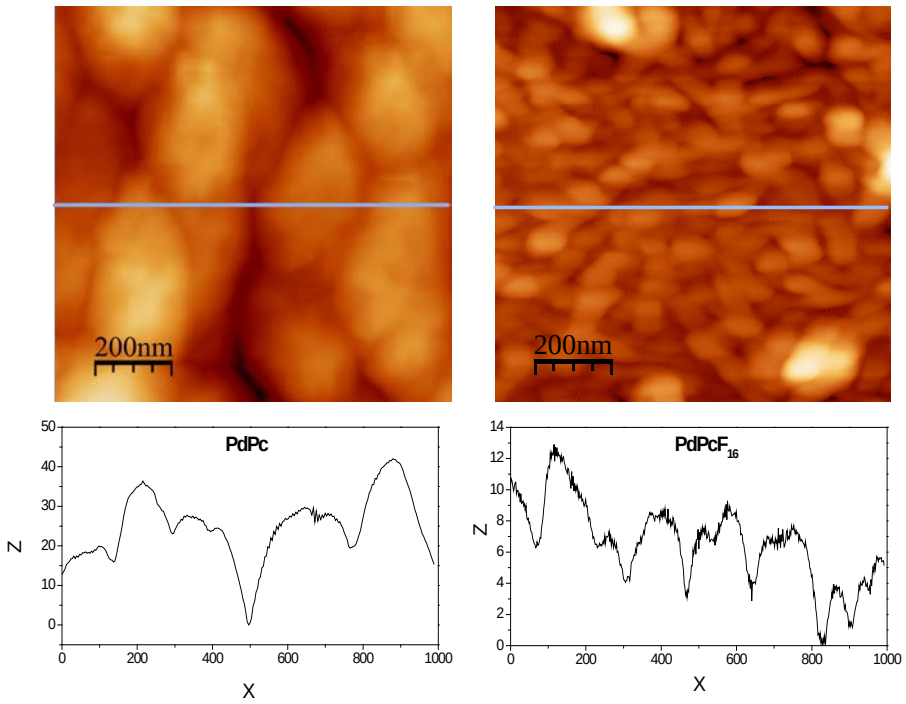

Figure 7. AFM images PdPc and $PdPcF_{16}$ thin films.

3.2. Study of sensor properties of the palladium phthalocyanine films

The sensitivity of thin films of PdPc and $PdPcF_{16}$ deposited onto interdigitated electrodes towards ammonia was measured by recording films' resistance as a function of time. Fig. 8 shows the curves representing a normalized sensor response R_n ($R_n = |R - R_o|/R_o$; where R is the steady resistance of the film at a certain analyte concentration and R_o is the baseline resistance of the film) of the PdPc and $PdFcF_{16}$ films on exposure to ammonia in the concentration range 10-50 ppm.

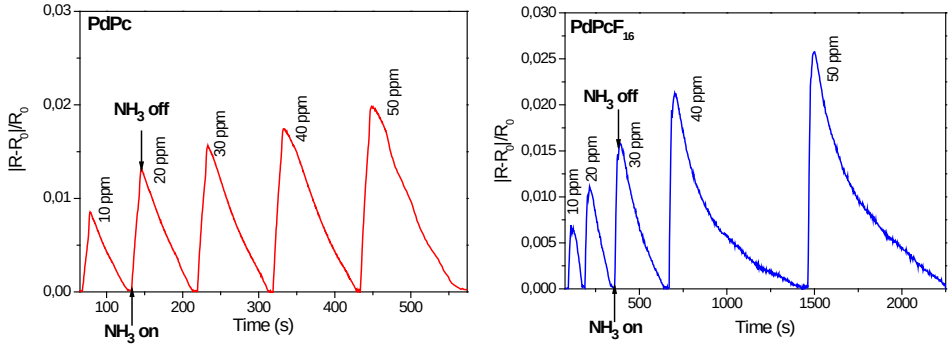

Figure 8. Normalized sensor response of PdPc and $PdFcF_{16}$ films on exposure to ammonia. Air was used as a diluting and purging gas.

Fig. 9 shows the sensor response of the same films on exposure to hydrogen in the concentration range 1000-5000 ppm. The PdPc and $PdPcF_{16}$ films demonstrate fully reversible sensor response both toward ammonia and hydrogen. However PdPc and $PdPcF_{16}$ films are not sensitive to low concentrations of hydrogen; the detection limits of hydrogen are about 400 ppm and 500 ppm in the case PdPc and $PdPcF_{16}$ films respectively.

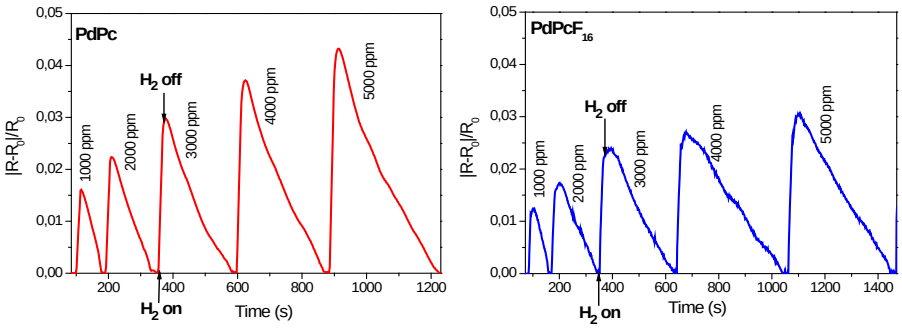

Figure 9. Normalized sensor response of PdPc and $PdFcF_{16}$ films on exposure to hydrogen. Air was used as a diluting and purging gas.

In the case of NH_3 detection, the recovery time is noticeably less for the PdPc film and rises from 50 to 120 s with increasing NH_3 concentration from 10 to 50 ppm. The recovery time of the $PdFcF_{16}$ films demonstrates much stronger dependence on NH_3 concentration; it changes from 55 to 750 s with increasing NH_3 concentration from 10 to 50 ppm.

In the case of H_2 detection, the recovery time is similar for both films and increases from 60 s to about 340 s with increasing hydrogen concentration from 1000 to 5000 ppm. It is worth mentioning here that purging the sensor gas cell with argon leads to irreversible sensor behavior whereas the sensor response is fully reversible on purging with air.

The sensor responses of PdPc films versus NH_3 and H_2 concentrations are depicted in Fig. 10 in comparison with that of the $PdPcF_{16}$ films, measured under the same experimental conditions.

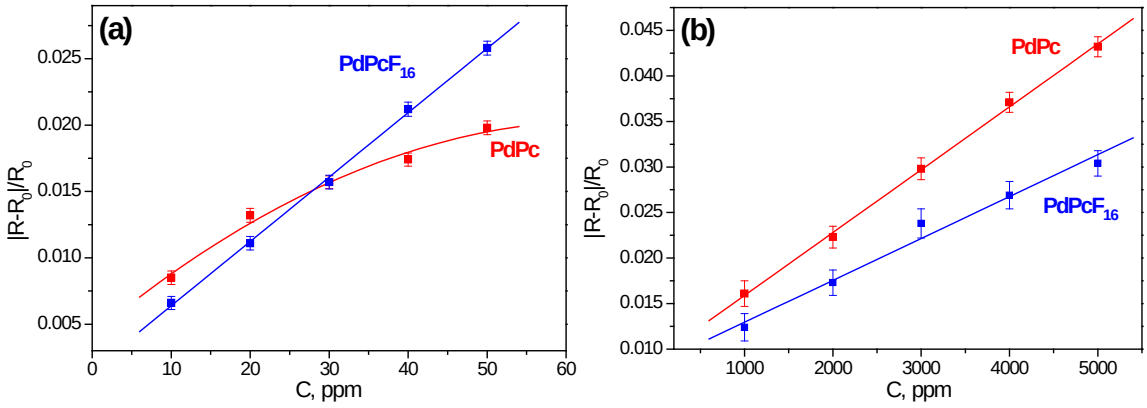

Figure 10. The dependence of the sensor response of PdPc and $PdFcF_{16}$ films on ammonia (a) and hydrogen (b) concentrations.

Fig. 10(a) shows that the sensor response toward ammonia is almost the same for both films in the NH_3 concentration range from 10 to 30 ppm, while that of the $PdPcF_{16}$ film rises markedly at higher NH_3 concentrations. The sensitivity of the PdPc film to hydrogen (Fig. 10) is slightly higher than that of the $PdPcF_{16}$ film.

In order to further understand the differences in the behavior of PdPc and $PdFcF_{16}$ films upon interaction with ammonia and hydrogen the DFT calculations have been performed.

3.3. Study of binding of ammonia and hydrogen to PdPc films

3.3.1. Experimental and theoretical study of vibrational spectra of palladium phthalocyanines

In order to check the validity of the theoretical calculations, we started from the detailed comparison of the predicted and experimental vibrational (IR and Raman) spectra of PdPc and $PcPcF_{16}$. Vibrational spectra of both PdPc derivatives have not been discussed in the literature. The experimental and calculated IR spectra of the studied PdPc forms are presented in Fig. 11. The experimental Raman spectra are given in Fig. S1 (Supplementary Information). A comparison of the experimental and calculated bands in the IR and Raman spectra of their assignments are given in the Tables S1-S4 (Supplementary Information). The experimentally measured vibrational wavenumbers of all molecules coincide well with DFT theoretical predictions. The RMS difference between the calculated and experimental wavenumbers was 20 cm^{-1}.

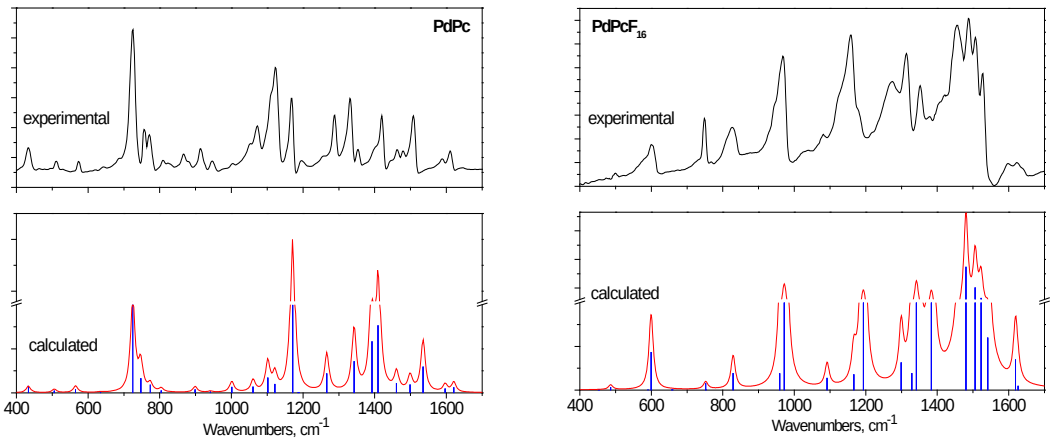

Figure 11. The experimental and calculated IR spectra of palladium phthalocyanines.

3.3.2. Theoretical study of ammonia binding to palladium phthalocyanines by DFT calculations

It is known that ammonia and amines interact with the central metal ion inside the phthalocyanine ring and form complexes with charge transfer from NH_3 to phthalocyanine molecule [14, 39, 40]. The binding of NH_3 molecule with PdPc and $PdPcF_{16}$ increases the out-of-

plane distortion in the Pc ring, because the NH_3 molecule binds with the Pd atom. It is reflected in an increase in the Pd-N_α bond length from 1.928 Å to 1.935 Å. The binding parameters for NH_3 with PdPc and $PdPcF_{16}$ are presented in Table 1. The calculated values of the binding energy E_b show that ammonia binds more strongly with $PdPcF_{16}$ than with PdPc. This fact appears to explain the larger recovery time of $PdPcF_{16}$-based sensors in comparison with PdPc-based ones.

Table 1. Parameters of the bond of NH_3 with PdPc and $PdPcF_{16}$

Compound	E_b, eV	d(Pd-NH_3), Å	q(NH_3), e	q(Pd), e	Q
PdPc⋯NH_3	-0,312	2,860	0,113	0,472	0,112
$PdPcF_{16}$⋯NH_3	-0,360	2,853	0,118	0,483	-1,912

At the same time the introduction of F-atoms in PdPc macrocycles causes a decrease of the bond length d(Pd-NH_3) between palladium atom and nitrogen atom of ammonia (Table 1). The increase in the bond strength between NH_3 and $PdPcF_{16}$ is caused by the increase in the electron density displacement from NH_3 to phthalocyanine through the central Pd atom. As a result NH_3 acquires a positive effective charge which is higher than in the case of PdPc. An increase of the positive charge q(Pd) of the Pd atom and the total negative charge Q of peripheral atoms of hydrogen or fluorine in the same sequence indicates the increase in the Pd atom acceptor properties in the case of $PdPcF_{16}$ derivative due to electron withdrawing properties of fluorine groups. This is reflected in the larger sensor response of $PdPcF_{16}$ films.

It is however worth remembering that the surface morphologies of PdPc and $PdPcF_{16}$ films are quite different from each other (Fig. 7) and that the film's morphology can also strongly influence the sensor behavior of these films. The rougher surface of the PdPc films with larger distances between the crystallites may induce faster adsorption/desorption rate of gaseous molecules.

3.3.3. Theoretical study of hydrogen binding to palladium phthalocyanines by DFT calculations

As a result of performing DFT calculations, it was shown that *V* orientation of hydrogen molecule relative to PdPc (Fig. 2) is the most preferable state. The dependence of interaction energy of H_2 with PdPc on the distance between palladium atom and the mass center of hydrogen molecule at its different orientations is presented in Fig. S2. The interaction energy for *V* orientation is approximately two times larger than in the case of P_1 and P_2 states. The dependences of E_i on d(Pd-H_2) in the case of $PdPcF_{16}$ are totally identical to those for PdPc. For *V* orientation the distance between the mass center of hydrogen molecule and palladium atom, which corresponds to the largest interaction energy, is approximately equal to 3.0 Å.

The considered structures of PdPc and $PdPcF_{16}$ with *V* oriented hydrogen molecule, which correspond to the largest interaction energies, were used as initial scenario for total geometry optimization to obtain the more accurate binding parameters of H_2, which are presented in Table 2.

Table 2. Parameters of the bond of H_2 with PdPc and $PdPcF_{16}$

Compound	E_b, eV	d(Pd-H_2), Å	q(H_2), *e*	q(Pd), *e*	*Q*
PdPc⋯H_2	-0,085	3,015	0,024	0,439	0,112
$PdPcF_{16}$⋯H_2	-0,083	3,015	0,026	0,453	-1,912

The small values of E_b, which only slightly exceed the energy of intermolecular interaction indicate the extremely weak binding of hydrogen molecules. The substitution of the peripheral hydrogen atoms by fluorine atoms weakly influences the parameters of the considered bond. The nature of the considered bond as well as in the case of NH_3 is based on the displacement of the electronic density from hydrogen molecule to phthalocyanines molecules through the palladium atom. That follows from the positive values of q(H_2), however these values are essentially small (0.024-0.026 *e*), and, perhaps, this fact causes the weak binding of hydrogen molecules to

palladium phthalocyanines. From this point of view the surface sorption of hydrogen itself may play some role in the hydrogen sensing behavior, nevertheless, it seems that the change in the resistance of MPc films upon interaction with H_2 has different mechanism from that in the case of ammonia and results from a gain of surface electrons following the reaction of hydrogen with adsorbed oxygen.

The resistance-based sensing mechanism of semiconducting sensors has been studied in the literature [41]. The commonly accepted mechanism is based on the variation of the surface electron depletion region due to the reaction between hydrogen and the chemisorbed oxygen on the surface. It has been assumed in the literature [42] that atmospheric oxygen absorbs at the air/MPc interface and at grain boundaries. It has been reported that the formation of charge-transfer complexes by coordination of O_2 to MPc at the air/phthalocyanine interface leads to the formation of oxidized MPc^+ and O_2^- species and injection of hole charge carriers into the film's bulk [43, 44]. The sensor layer is then exposed to hydrogen atmosphere and the hydrogen molecules react with the adsorbed oxygen species. The redox reaction is exothermic and results in the fast desorption of produced H_2O molecules from the surface [45]. Due to the released electrons a change of the resistance of the semiconductor is observed.

Taking into account this possible resistance-based sensing mechanism, the additional quantum-chemical calculations were carried out by the same method, where the binding of an O_2 molecule with PdPc was studied as an intermediate step before an interaction with H_2 molecule. It was shown that the nature of the considered bond completely differs from that between phthalocyanine and NH_3 or H_2 molecules. First of all it depends on the spin state of palladium phthalocyanine, therefore, in the singlet spin state of PdPc the oxygen molecule is bonded by the nitrogen atom of one of the pyrrole cycles (Fig. 12 left) and becomes positively charged (0.019 *e*), which means that electron density moves from O_2 molecule onto the macrocycle. The binding energy in this case is equal to -0.185 eV. In the triplet spin state of PdPc the oxygen molecule is bonded by the nitrogen atom linking two pyrrole cycles (Fig. 12 right) and becomes

negatively charged (-0.134 *e*), which agrees with the experimental observations. In this case the binding energy is equal to -0.360 eV.

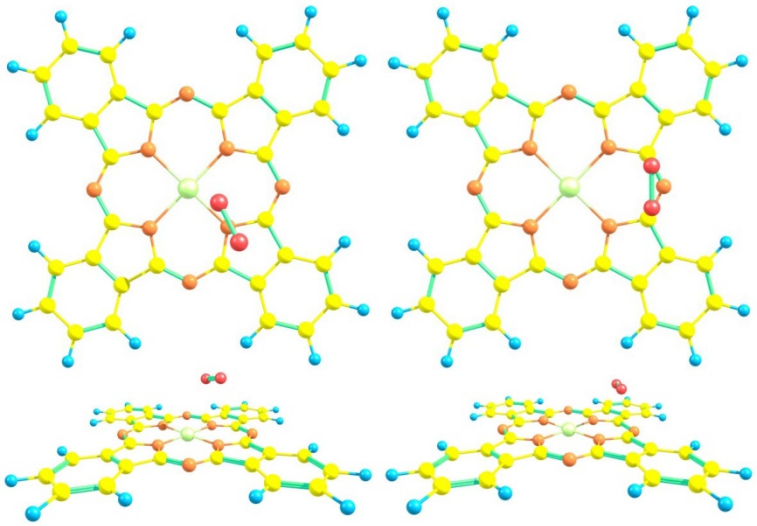

Figure 12. The geometries of the palladium phthalocyanine complexes with the oxygen molecule at the singlet spin state (left) and triplet spin state (right) of PdPc.

It follows that in both cases of spin states of the palladium phthalocyanine the strength of the oxygen molecule binding is much higher than that of the hydrogen molecule; this means that the first type of binding is more preferable than the second one. In this case H_2 molecules can interact directly with $PdPc^{+}O_2^{-}$ complex that leads to desorption of the oxygen molecule in the form of H_2O molecules. This process is quite possible at the normal conditions because the calculated change of the free Gibbs energy here is negative and equal to -369 $kJ \cdot mol^{-1}$ for both cases of spin states. As a result of oxygen desorption a change of the resistance of the semiconducting PdPc films is observed.

Conclusions

The structure and sensor response of thin films of unsubstituted and hexadecafluorosubstituted palladium phthalocyanines were studied and compared. Thin films of PdPc and $PdPcF_{16}$ were obtained by means of organic molecular beam deposition and their

structure was studied using UV-visible spectroscopy, X-ray diffraction and atomic force microscopy techniques. Using XRD method the PdPc powder was identified as α-PdPc phase with the triclinic unit cell. The resulting unit cell parameters for α-PdPc are: a = 12.19(8) Å; b =3.74(3) Å; c = 13.8(1) Å; α = 107.42(1)°; β = 96.84(1)°; γ = 81.39(1)°; V = 591.74 $Å^3$. PdPc thin layers have a strong preferred orientation, with the plane (001) oriented parallel to the substrate plane. The diffraction pattern from the polycrystalline $PdPcF_{16}$ sample is significantly different from α-PdPc, indicating a significant change in its crystalline structure. The surface morphology of PdPc and $PdPcF_{16}$ films was also quite different, with the grain size in the PdPc films in the region of 150–220 nm. On the other hand the surface of $PdPcF_{16}$ films consisted of much smaller particles with a diameter no more than 100 nm.

Sensitivity of PdPc and $PdPcF_{16}$ films towards ammonia (10-50 ppm) and hydrogen (1000-5000 ppm) was measured by continuously recording films' resistance. The PdPc and $PdPcF_{16}$ films demonstrate full reversible sensor response both toward ammonia and hydrogen. The value of sensor response toward ammonia is almost the same for both films in the NH_3 concentration range 10-30 ppm, while $PdPcF_{16}$ film exhibited markedly enhanced response at higher NH_3 concentrations. The sensitivity of the PdPc film to hydrogen is slightly higher than that of the $PdPcF_{16}$ film.

The nature and parameters of chemical binding between PdPc derivatives and analyte molecules were described by quantum-chemical calculations utilizing DFT method. Ammonia interacts with the central metal ion inside the phthalocyanine ring and forms complexes with charge transfer from NH_3 to phthalocyanine molecule. The calculated values of binding energy show that NH_3 binds more strongly with $PdPcF_{16}$ than with PdPc.

The small values of binding energy, which only slightly exceed the energy of intermolecular interaction indicate the extremely weak binding of hydrogen molecules with PdPc. It seems that the change of MPc films resistance upon interaction with H_2 has different mechanism from that

occurring in the case of ammonia and results from a gain of surface electrons following the reaction of hydrogen with adsorbed oxygen.

Acknowledgements

This work was supported by the Russian Science Foundation (project N 15-13-10014).

References

1. Simic-Glavaski B. *Phthalocyanines, Properties and Applications Vol. 3;* VCH: New York, USA, 1993.

2. Karl N., Kraft K. H., Marktanner J., Münch M., Schatz F., Stehle R., Uhde H. M. Fast electronic transport in organic molecular solids? *J. Vac. Sci. Technol. A.* **1999**, 17, 2318-2328.

3. Kim I., Haverinen H. M., Wang Z., Madakuni S., Li J., Jabbour G. E. Effect of molecular packing on interfacial recombination of organic solar cells based on palladium phthalocyanine and perylene derivatives. *Appl. Phys. Lett.* **2009**, 95, 023305.

4. Signerski R., Jarosz G., Koscielska B. On photovoltaic effect in hybrid heterojunction formed from palladium phthalocyanine and titanium dioxide layers. *J. Non-Crystalline Solids* **2009**, 355, 1405-1407.

5. Jarosz G. On small signal capacitance spectra of organic diode formed by ITO–palladium phthalocyanine–Al sandwich system. *Thin Solid Films* **2010**, 518, 4015-4018.

6. Jafari M. J., Azim-Araghi M.E., Barhemat S. Effect of chemical environments on palladium phthalocyanine thin film sensors for humidity analysis. *J. Mater. Sci.* **2012**, 47, 1992-1999.

7. Azim-Araghi M. E., Karimi-Kerdabadi E., Jafari M. J. Optical and electrical properties of nanostructured heterojunction (Au|PdPc|ClAlPc|Al) and using as O_2 sensor. *Eur. Phys. J. Appl. Phys.* **2011**, 55, 30203-30211.

8. Jafari M. J., Azim-Araghi M. E., Barhemat S., Riyazi S. Effect of post-deposition annealing on surface morphology and gas sensing properties of palladium phthalocyanine thin films. *Surf. Interface Anal.* **2012**, 44, 601-608.

9. Jakubik W. P., Urbanczyk M. W., Kochowski S., Bodzenta J., Palladium and phthalocyanine bilayer films for hydrogen detection in a surface acoustic wave sensor system. *Sens. Actuators B: Chem.* **2003**, 96, 321-328.

10. Jakubik W., Urbanczyk M., Maciak E. Metal-free phthalocyanine and palladium sensor structure with a polyethylene membrane for hydrogen detection in SAW systems. *Sens. Actuators B: Chem.* **2007**, 127, 295-303.

11. Jakubik W. Sensor properties of bilayer structures with palladium, lead and cobalt phthalocyanines in surface acoustic wave and electric systems. *Mol. Quantum Acoust.* **2004**, 25, 141-152.

12. Hübert T., Boon-Brett L., Black G., Banach U., Hydrogen sensors – A review. *Sens. Actuators B: Chem.* **2011**, 157, 329-352.

13. Basova T., Kol'tsov E., Hassan A., Tsargorodskaya A., Ray A., Igumenov I., Thin films of copper hexadecafluorophthalocyanine $CuPcF_{16}$. *Phys. Stat. Sol. (b).* **2005**, 242, 822–827.

14. Klyamer D. D., Sukhikh A. S., Krasnov P. O., Gromilov S. A., Morozova N. B., Basova T. V. Thin films of tetrafluorosubstituted cobalt phthalocyanine: Structure and sensor properties. *Appl. Surf. Sci.*, **2016**, 372, 79-86.

15. Handa M., Suzuki A., Shoji S., Kasuga K., Sogabe K. Spectral and electrochemical properties of vanadyl hexadecafluorophthalocyanine. *Inorg. Chim. Acta* **1995**, 230, 41-44.

16. Hesse K., Schlettwein D. Spectroelectrochemical investigations on the reduction of thin films of hexadecafluorophthalocyaninatozinc ($F_{16}PcZn$). *J. Electroanal. Chem.*, **1999**, 476, 148-158.

17. Ma X., Chen H., Shi M., Wu G., Wang M., Huang J., High gas-sensitivity and selectivity of fluorinated zinc phthalocyanine film to some non-oxidizing gases at room temperature. *Thin Solid Films* **2005**, 489, 257-261.

18. Basova T., Kiselev V., Dubkov I., Latteyer F., Gromilov S., Peisert H., Chassé T. Optical Spectroscopy and XRD Study of Molecular Orientation, Polymorphism, and Phase Transitions in Fluorinated Vanadyl Phthalocyanine Thin Films. *J. Phys. Chem. C* **2013**, 117, 7097-7106.

19. Yang J., Yim S., Jones T. S. Molecular-Orientation-Induced Rapid Roughening and Morphology Transition in Organic Semiconductor Thin-Film Growth. *Scientific Reports* **2015**, 5, 9441.

20. Schuster B., Basova T., Plyashkevich V., Peisert H., Chassé T. Effects of temperature on structural and morphological features of CoPc and $CoPcF_{16}$ thin films. *Thin Solid Films* **2010**, 518, 7161-7166.

21. de Oteyza D. G., Barrena E., Zhang Y., Krauss T. N., Turak A., Vorobiev A., Dosch H. Experimental Relation between Stranski−Krastanov Growth of DIP/F_{16}CoPc Heterostructures and the Reconstruction of the Organic Interface. *J. Phys. Chem. C* **2009**, 113, 4234-4239.

22. Sukhikh A.S., Basova T.V., Gromilov S.A. Development of X-ray studies technique of thin layers on an example of cobalt phthalocyanine. *J. Struct. Chem.* **2016**, 57, 618-621 doi:10.1134/S0022476616030227.

23. Becke A. D. Density-functional exchange energy approximation with correct asymptotic behavior. *Phys. Rev. A* **1988**, 88, 3098-3100.

24. Perdew J. P. Density functional approximation for the correlation energy of the inhomogeneous electron gas. *Phys. Rev. B* **1986**, 33, 8822-8824.

25. Schaefer A., Horn H., Ahlrichs R. Fully optimized contracted Gaussian basis set for atoms Li to Kr. *J. Chem. Phys.* **1992**, 97, 2571-2577.

26. Schaefer A., Huber C., Ahlrichs R. Fully optimized contracted Gaussian basis set of triple zeta valence quality for atoms Li to Kr. *J. Chem. Phys.* **1994**, 100, 5829-5835.

27. Grimme S., Ehrlich S., Goerigk L. Effect of the Damping Function in Dispersion Corrected Density Functional Theory. *J. Comput. Chem.* **2011**, 32, 1456-1465.

28. Grimme S., Antony J., Ehrlich S., Krieg H. A consistent and accurate ab initio parametrization of density functional dispersion correction (DFT-D) for the 94 elements H-Pu. *J. Chem. Phys.* **2010**, 132, 154104.

29. Neese F. The ORCA program system, *WIREs Comput. Mol. Sci.* **2012**, 2, 73-78.

30. Kasha M., Rawls H. R., El-Bayoumi M. A. The excition model in molecular spectroscopy. *Pure Appl. Chem.* **1965**, 11, 371-392.

31. Engel M. K. *Single-Crystal Structures of Phthalocyanine Complexes and Related Macrocycles, in: The Porphyrin Handbook, Vol. 20*; Academic Press: Houston, USA, 2002.

32. Schlettwein D., Hesse K., Tada H., Mashiko S., Storm U., Binder J. Ordered Growth of Substituted Phthalocyanine Thin Films: Hexadecafluorophthalocyaninatozinc on Alkali Halide (100) and Microstructured Si Surfaces. *Chem. Mater.* **2000,** 12, 989-995.

33. Schlettwein D., Graaf H., Meyer J.-P., Oekermann T., Jaeger N. I. Molecular Interactions in Thin Films of Hexadecafluorophthalocyaninatozinc (F_{16}PcZn) as Compared to Islands of N,N‘-Dimethylperylene-3,4,9,10-biscarboximide (MePTCDI). *J. Phys. Chem. B* **1999**, 103, 3078-3086.

34. Michaelis W., Wöhrle D., Schlettwein D. Organic n-channels of substituted phthalocyanine thin films grown on smooth insulator surfaces for organic field effect transistors applications *J. Mater. Res.* **2004**, 19, 2040-2048.

35. Schlettwein D., Tada H., Mashiko S. Substrate-Induced Order and Multilayer Epitaxial Growth of Substituted Phthalocyanine Thin Films. *Langmuir* **2000**, 16, 2872-2881.

36. Kempa A., Dobrowolski J. Palladium phthalocyanine and its polymorphic forms. *Can. J. Chem.* **1988**, 66, 2553-2555

37. Boultif A., Louer D. Powder pattern indexing with the dichotomy method. *J. Appl. Cryst.* **2004**, 37, 724-731.

38. Werner P.-E., Eriksson L., Westdahl M. Treor, a semi-exhaustive trial-and-error powder indexing program for all symmetries. *J. Appl. Cryst.* **1985**, 18, 367-370.

39. Paolesse R., Di Natale C., Dall'Orto V. C., Macagnano A., Angelaccio A., Motta N., Sgarlata A., Hurst J., Rezzano I., Mascini M., D'Amico A. Porphyrin thin films coated quartz crystal microbalances prepared by electropolymerization technique. *Thin Solid Films* **1999**, 354, 245-250;

40. Basova T. V., Hassan A., Krasnov P. O., Gürol I., Ahsen V. Trimethylamine Sorption into Thin Layers of Fluoroalkyloxy and Alkyloxy Substituted Phthalocyanines: Optical Detection and DFT Calculations. *Sens. Actuators B: Chem.* **2015**, 216, 204-211.

41. Soundarrajan P., Schweighardt F. *Hydrogen Sensing and Detection, in: Hydrogen Fuel. Production, Transport, and Storage;* CRC Press: Boca Raton, USA, 2008.

42. Gould R. D. Structure and electrical conduction properties of phthalocyanine thin films. *Coord. Chem. Rev.* **1996**, 156, 237-274.

43. Kerp H. R., Westerdui K. T., van Veen A. T., van Faassen E. E. Quantification and effects of molecular oxygen and water in zinc phthalocyanine layers. *J. Mater. Res.* **2001**, 16, 503-511.

44. de Haan A., Debliquy M., Decroly A. Influence of atmospheric pollutants on the conductance of phthalocyanine films. *Sens. Actuators B: Chem.* **1999**, 57, 69-74.

45. Gu H., Wang Z., Hu Y. Hydrogen Gas Sensors Based on Semiconductor Oxide Nanostructures. *Sensors* **2012**, 12, 5517-5550.